Orientation and Stabilization of Dual Spin Satellites Using Aerodynamic Torque

P. A. Finlayson[1] and C. D. Clayton[2]

INTRASPACE CORPORATION
North Salt Lake City, Utah

Abstract

Nadir pointing satellites can experience large atmospheric torques during low perigee parking orbits. Countering these torques can quickly saturate the momentum wheels or consume unacceptable amounts of reaction gas, making earth pointing near perigee impossible or impractical. This paper describes a technique which allows dual momentum wheel spacecraft to exploit this aerodynamic torque to achieve a stable, aerodynamically neutral orientation. In addition, this torque, coupled with the spacecraft gyro-dynamics and orbit rate, results in a natural alignment of the momentum wheel bias vector with the orbit plane normal. From this known orientation, returning to nadir pointing is simple, requiring only a 90° rotation around the pitch axis. Nutation damping and longitudinal stability are achieved by torquing the momentum wheels using a simple control law.

Background

The INTRASPACE T-36 spacecraft is shown in Figures 1 and 2. The satellite is equipped with a cold gas (N2) attitude control system, canted momentum wheels, magnetic torque rods, and an internal booster motor. Attitude orientation is monitored with a sun sensor, a triple sensor earth detector, and rate gyros. The deployed solar panels and high accuracy earth pointing attitude control mechanisms are designed for normal operational conditions in a circulate 800 km orbit. However, in route to its final orbit it must operate for several days in a lower, 200 km x 600 km orbit, before boosting itself to its final altitude.

At perigee of the intermediate orbit the spacecraft will be subjected to significant atmospheric drag forces which can degrade the orbit altitude and create torques which can require significant amounts of onboard fuel to counteract. The operational mode described in this paper, temporarily aligns the spacecraft longitudinal axis with the velocity vector to minimize the effects of drag on the orbit altitude and spacecraft attitude. Orientation stability is achieved by applying a control law to the operation of the momentum wheels.

Introduction and Summary

This paper presents a solution to the problem of high aerodynamic drag and resulting aerodynamic torque encountered by the T-36 spacecraft during the 200 km x 600 km orbit delivered by the SCOUT launch vehicle.

The initial mission design required that the T-36 spacecraft maintain nadir pointing while in the 200 km x 600 km orbit delivered by the SCOUT launch vehicle. Recent analysis, however, has shown that the predicted aerodynamic torque experienced by the spacecraft near perigee would be much too high for this strategy to be practical. Maintaining nadir pointing using the momentum wheels would quickly result in saturation, and maintaining nadir pointing using cold gas thrusters would consume N_2 at an unacceptable rate.

---

[1]Director of Analysis
[2]Manager, Spacecraft Subsystems

curve fit to provide the following analytic expression for density as a function of spacecraft altitude:

$$\rho = \exp\left(-\left[a_0 + a_1 h + a_2 h^2\right]\right)$$

where

a_0 = 17.26964218181818
a_1 = 0.02784455069049
a_2 = -0.00001481310123

and

h = Spacecraft altitude (km)
r = Atmospheric density (kg/m^3)

Figure 3 shows a plot of the analytic expression and the actual data points.

Aerodynamic Force and Torque Model

The aerodynamic force and torque on the T-36 spacecraft are calculated by integrating the differential contributions over the surface of the spacecraft. This integration can be performed analytically for the spacecraft cylinder and the circular cylinder ends. The panels are assumed flat for this analysis (with an area equal to their normal projection). Geometry calculations determine the portion of the panels which are shielded from air molecules by a "wind shadow" cast by the cylinder or an opposite panel. These shielded areas do not contribute to drag force or moment.

The differential force vector produced by atmospheric drag on a differential area is given by (Wertz, section 17.2.3):

$$d\mathbf{F} = -\frac{1}{2} C_D \rho v^2 (\hat{\mathbf{n}} \bullet \hat{\mathbf{v}}) \hat{\mathbf{v}} dA$$

where:

$d\mathbf{F}$ = Differential drag force vector
$\hat{\mathbf{n}}$ = Unit vector normal to the surface element dA
$\hat{\mathbf{v}}$ = Unit vector in velocity vector direction
v = Velocity magnitude
C_D = Drag coefficient

This model is based upon an inelastic molecular impact model (no reflection). Wertz recommends a drag coefficient value of 2.0 where no measured data is available. To be conservative, a value of 2.2 is used for this analysis.

The differential torque vector produced by atmospheric drag on a differential area is given by:

$$d\mathbf{N} = \mathbf{r}_{cm} \mathbf{x}\, d\mathbf{F}$$

where

$d\mathbf{N}$ = Differential drag torque vector

$\mathbf{r}_{cm}$ = Vector from center of mass to element
$d\mathbf{F}$ = Differential drag force vector

Figure 4 shows a diagram of the T-36 spacecraft with labeled dimensions and drag regions. Figure 5 shows scaled aerodynamic torque for the five different drag regions of the spacecraft as a function of angle of attack (the angle between the -Z axis and the velocity vector). The torque is scaled so that it is independent of velocity magnitude. Figure 6 shows computed total drag force and total drag torque as functions of angle of attack for the particular case of 185 km spacecraft altitude.

Momentum Wheel Control Law

Aerodynamic forces provide a natural torque in a direction which tends to restore the spacecraft to a zero angle of attack. However, there is very little natural damping on the system and oscillations would tend to continue indefinitely. To illustrate this effect, Figure 7 shows simulated pitch response vs. time for an initial 1° pitch angle with no damping control in a 200 km circular orbit. This shows a natural frequency of about one cycle per 200 seconds. Figure 8 shows the corresponding yaw response vs. time for an initial yaw error of 1°. For this plot the momentum wheels are running at a constant nominal value of 2 N-m-s in the -Y direction (no control law is active). The natural frequency for the yaw/roll response is about one cycle per 1500 seconds. (With the wheels off, the yaw response would be about the same as the pitch response.) The natural nutation response can also bee seen in Figure 8 as a higher frequency oscillation on top of the main curve. By using an active control law to torque the momentum wheels, the pitch and yaw/roll oscillations (as well as the nutation) can be effectively damped out. The control law attempts to damp out oscillations of the spacecraft while maintaining a desired level of angular momentum stored in the wheels.

The damping control law developed for the Aero-neutral mode is of the form:

$$\dot{h}_y = k_1\left(\omega_y + \omega_{orbit}\right) - k_2\left(h_y - h_{y0}\right)$$
$$\dot{h}_z = k_3\omega_z - k_4 h_z$$

$$\dot{h}_1 = \frac{1}{2}\left(\frac{\dot{h}_z}{\sin\alpha} - \frac{\dot{h}_y}{\cos\alpha}\right)$$
$$\dot{h}_2 = -\frac{1}{2}\left(\frac{\dot{h}_z}{\sin\alpha} + \frac{\dot{h}_y}{\cos\alpha}\right)$$

where

ω_y = Angular rate about Y axis
ω_z = Angular rate about Z axis
ω_{orbit} = Mean orbit rate
h_y = Y axis component of wheel angular momentum
h_z = Z axis component of wheel angular momentum
h_{y0} = Nominal Y axis component of wheel angular momentum
α = Angle between Y axis and wheel axes
$\dot{h}_1$ = Torque command to wheel 1

$\dot{h}_2$ = Torque command to wheel 2
k_1, k_2, k_3, k_4 = Control law gains

Figures 9 and 10 show angular responses to the same initial conditions as those for Figures 7 and 8, but with the above control law active. Figures 11 and 12 show response to an arbitrarily chosen set of large initial orientation angles. Figure 11 shows the response with momentum wheel control law damping, while Figure 12 shows response for the same initial conditions, but with no control law active. As with the previous example, this is for a 200 km circular orbit.

Aero-neutral Mode Performance (200 km x 600 km Orbit)

Figures 13 through 16 show orbital simulations for several orbits with initial conditions imposed at apogee. For Figures 13 and 14 the arbitrarily chosen initial conditions are: Yaw = -22°, Pitch = -5°, and Roll = 13°. For this simulation, no Z axis torques were generated. The final simulation run included (Figures 15 through 16) include a Z axis torque proportional to the Y axis torque produced by one of the solar panels. For this simulation the initial conditions are: Yaw = 41°, Pitch = -25°, and Roll = 53°. For all of these Figures, the time axis is in units of orbits, with the integral values at apogee (since this was chosen for the initial conditions) and half-integral values being perigee. The plots shown are representative of the many simulations run (some with randomly chosen initial conditions). In all cases, the initial angular orientation converged in a stable manner to an equilibrium pattern. For this pattern, Yaw and Roll maintain small values while Pitch goes through a repeating pattern with somewhat larger excursions from zero. The pitch pattern depends upon the eccentricity of the orbit and how quickly the atmospheric density falls off as the spacecraft climbs towards apogee.

Conclusions

By allowing the satellite to pass through perigee at zero angle of attack, drag forces are minimized, and the attitude oscillations are controllable and can be damped using active control with the momentum wheels. This technique has the additional advantage that the bias momentum vector created by the momentum wheels naturally aligns itself normal to orbit plane. This simplifies subsequent earth acquisition.

References

Wertz, James R., *Spacecraft Attitude Determination and Control* , D. Reidel Publishing Company, Dordrecht, Holland, 1979.

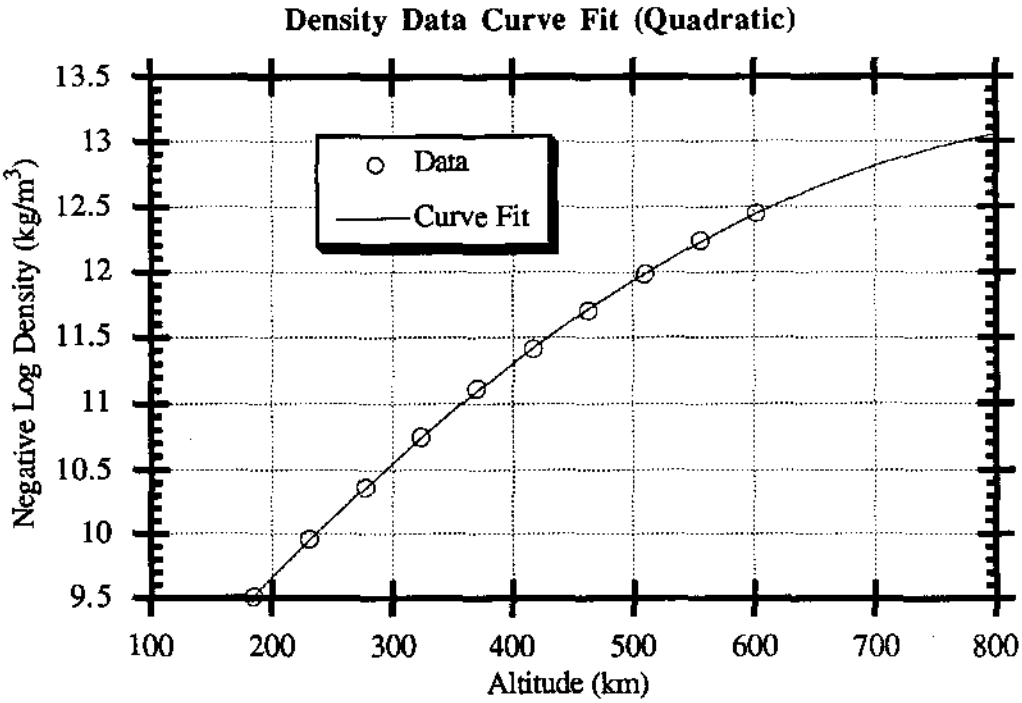

Figure 3 - Density Curve Fit Plot

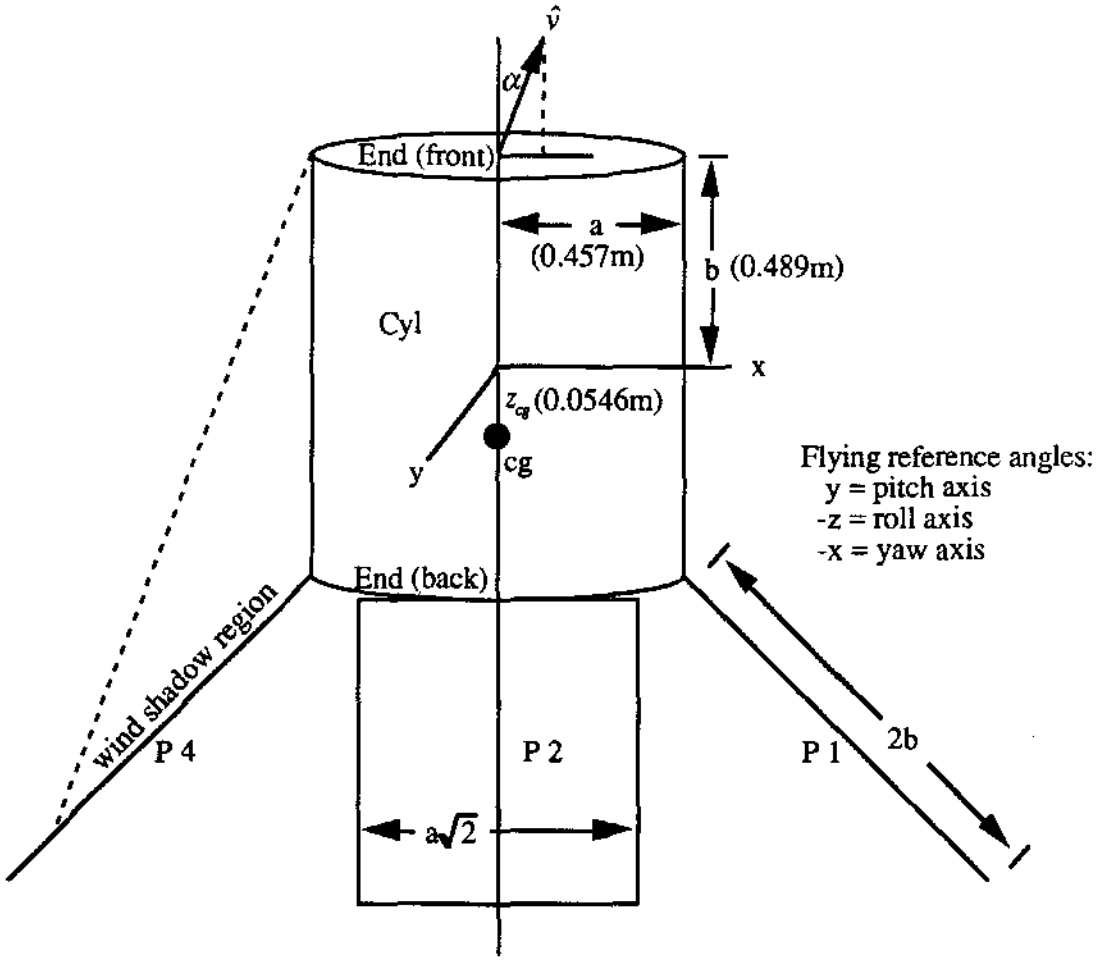

Figure 4 - T-36 Spacecraft Diagram

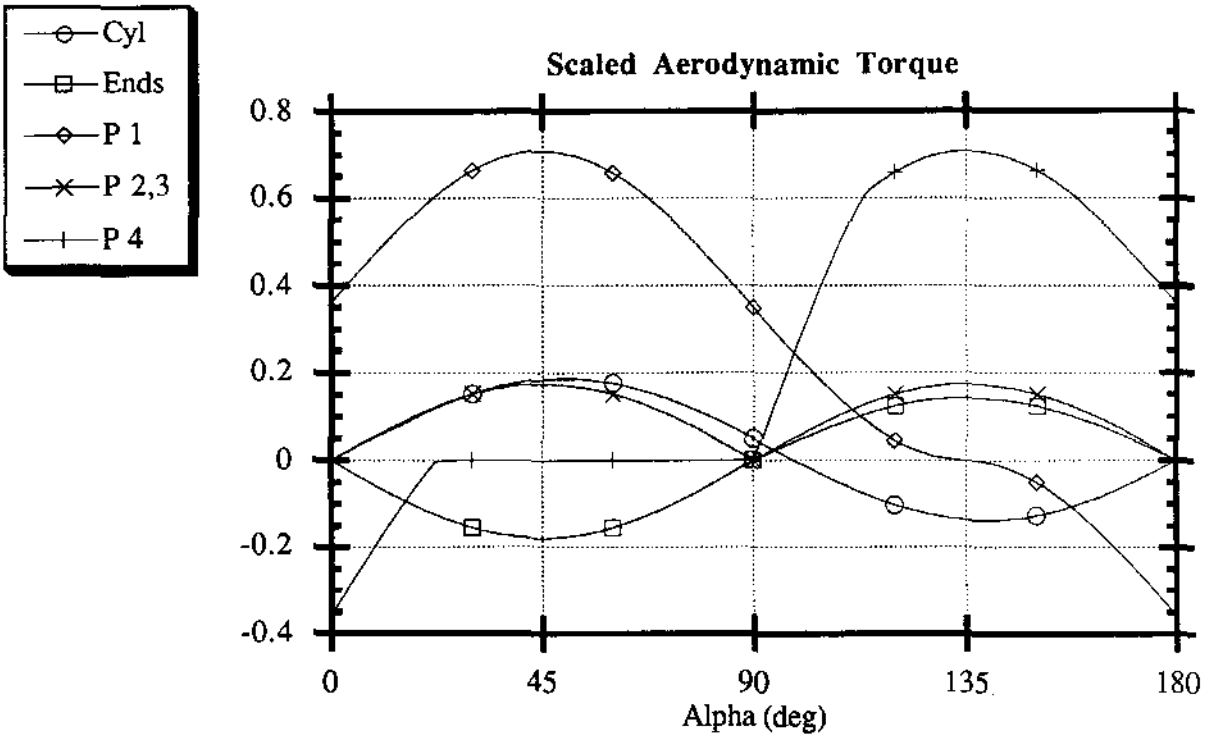

Figure 5 - Scaled Aerodynamic Torque vs. Angle of Attack

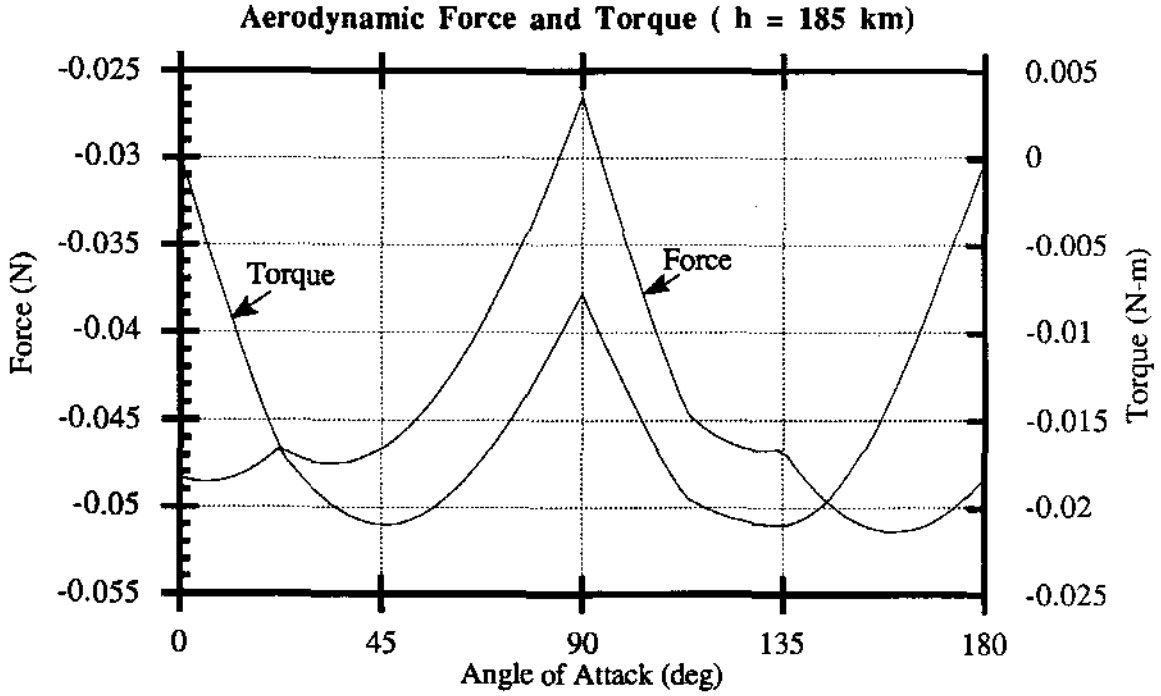

Figure 6 - Drag Force and Torque vs. Angle of Attack

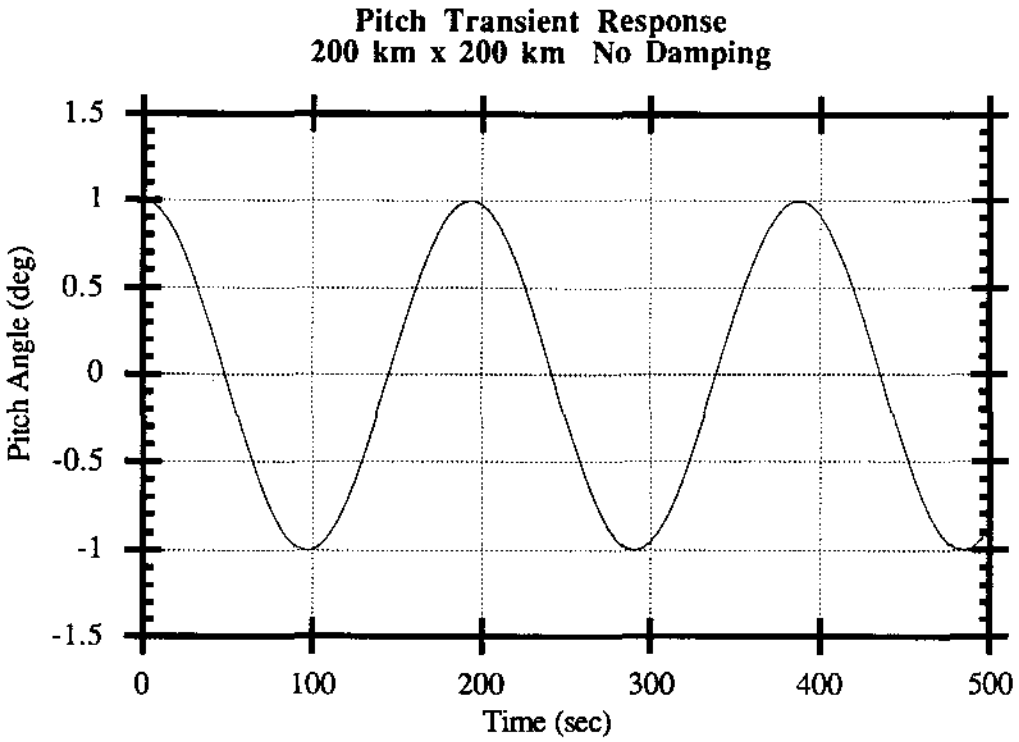

Figure 7 - Undamped Pitch Response

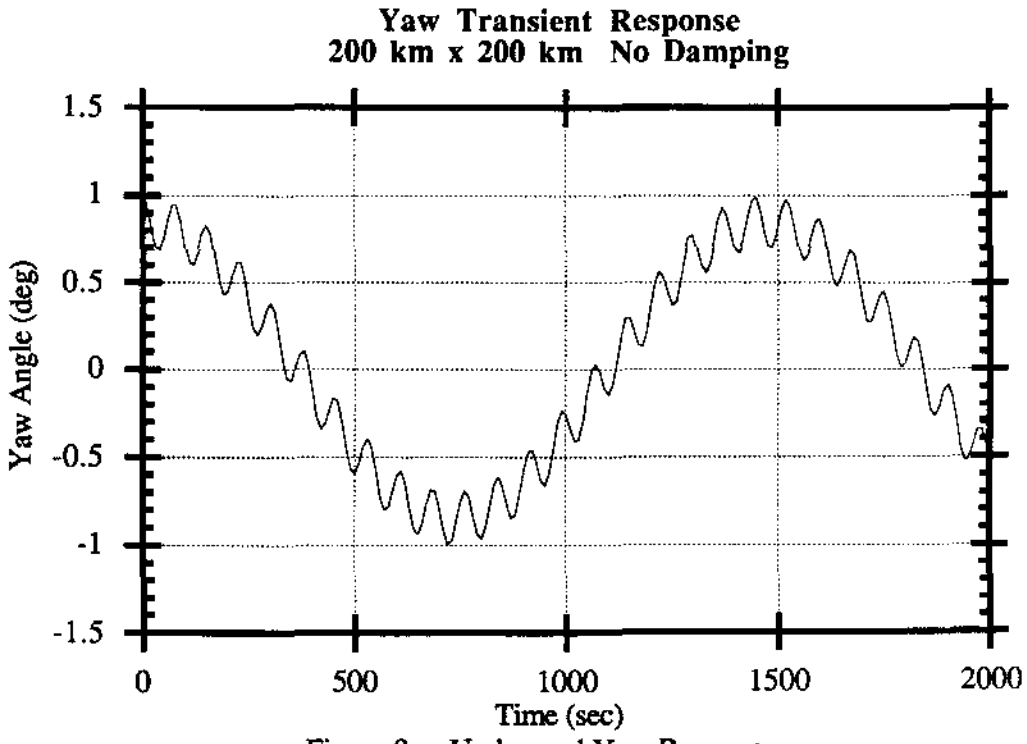

Figure 8 - Undamped Yaw Response

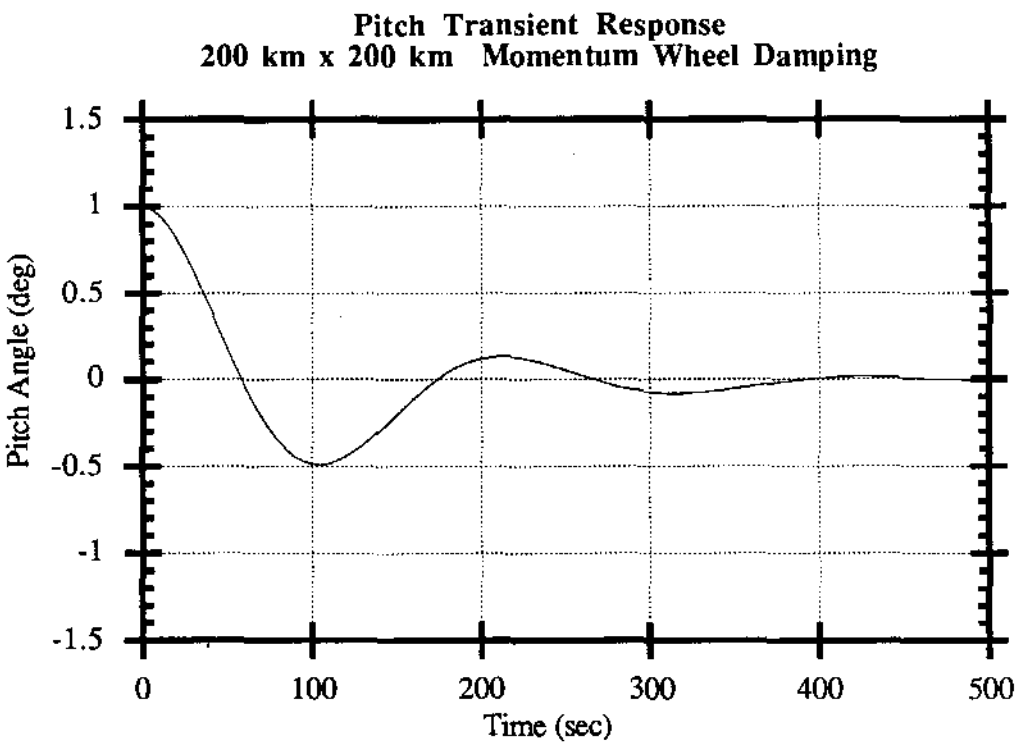

Figure 9 - Damped Pitch Response

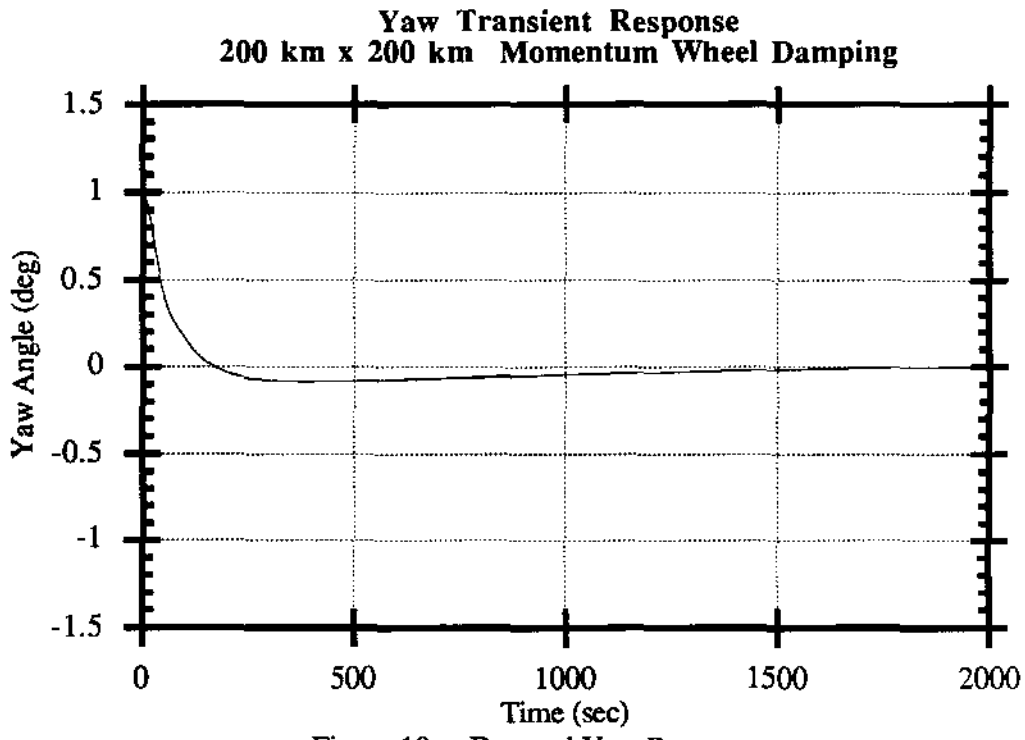

Figure 10 - Damped Yaw Response

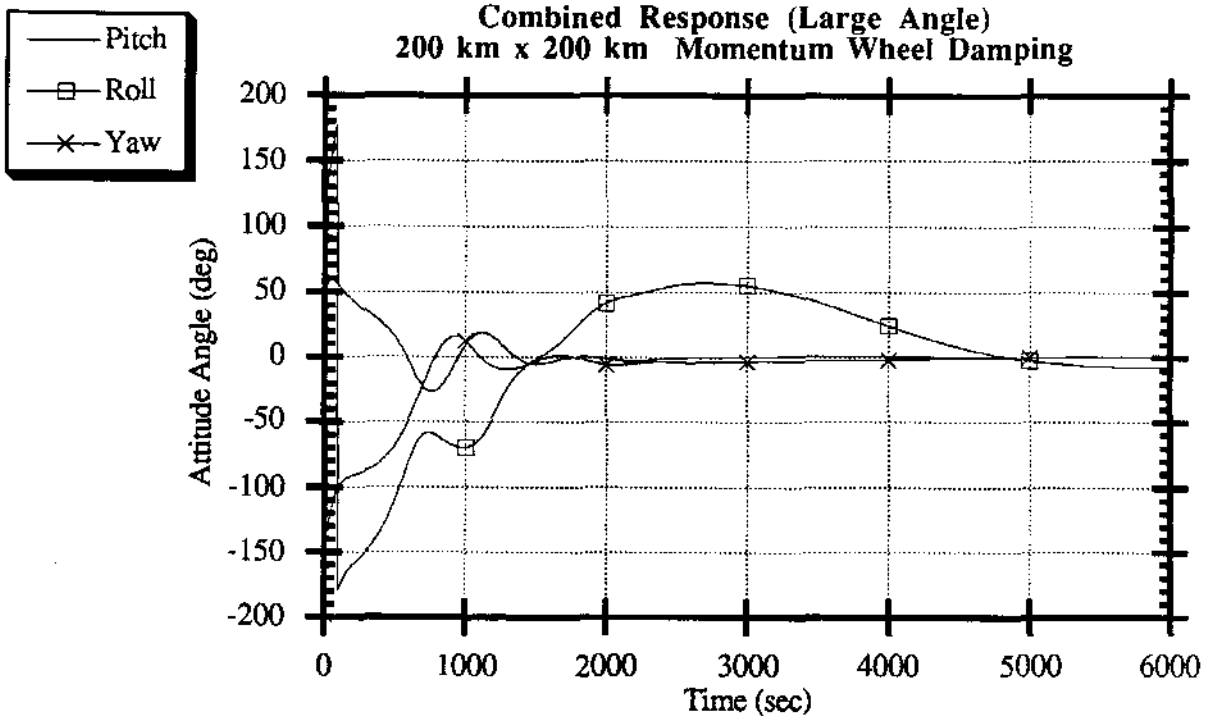

Figure 11 - Attitude Response With Damping

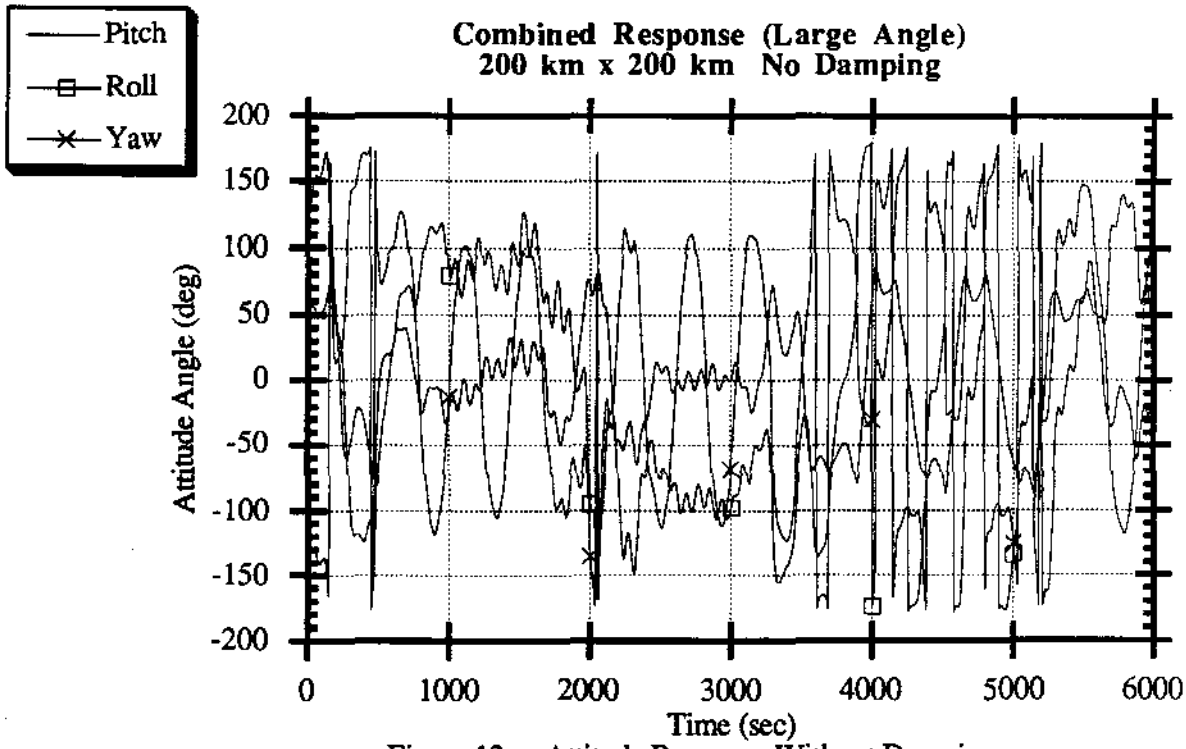

Figure 12 - Attitude Response Without Damping

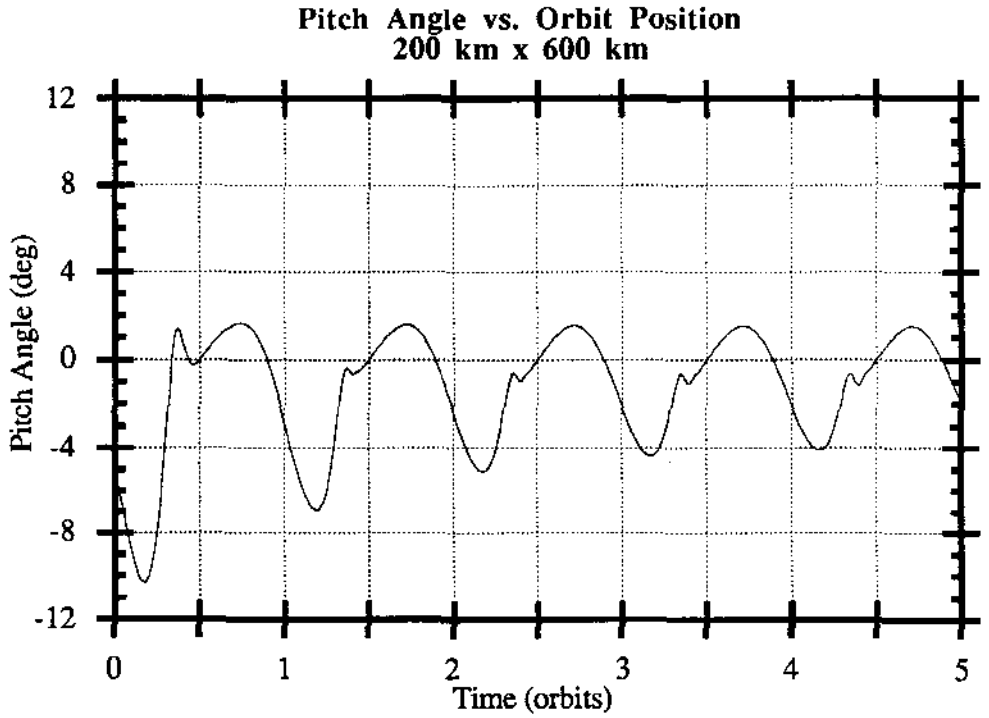

Figure 13 - Pitch Response vs. Time

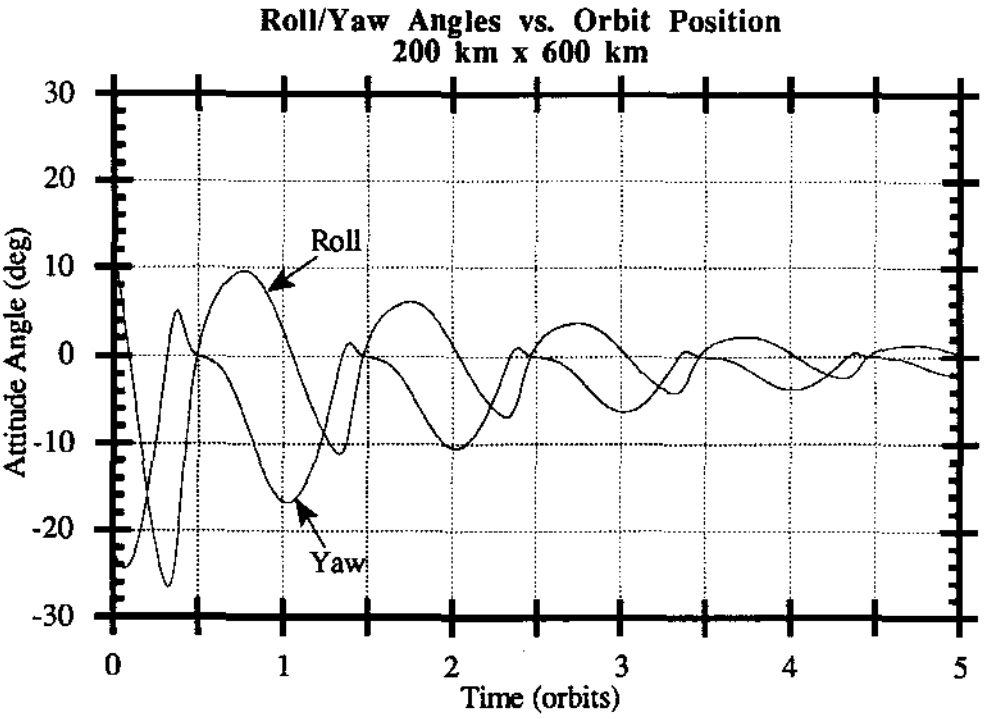

Figure 14 - Roll/Yaw Response vs. Time

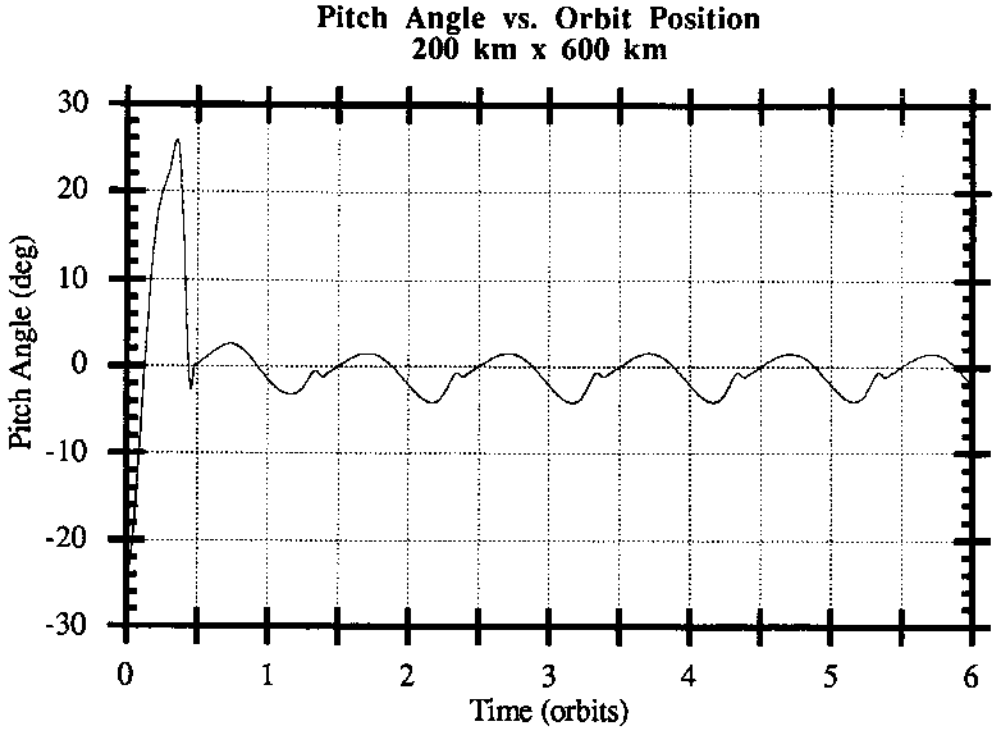

Figure 15 - Pitch Response vs. Time

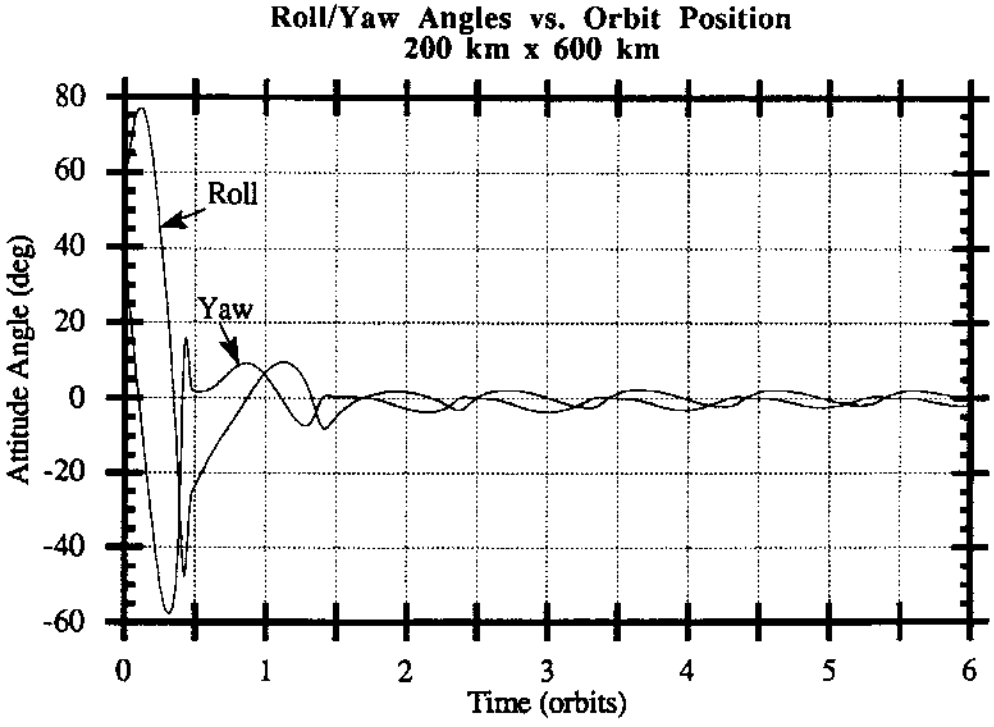

Figure 16 - Roll/Yaw Response vs. Time